Development 137, 261-271 (2010) doi:10.1242/dev.039636

VEGF is required for dendritogenesis of newly born olfactory bulb interneurons

Tamar Licht[1,*], Ronen Eavri[1,*], Inbal Goshen[1], Yael Shlomai[2], Adi Mizrahi[2,†] and Eli Keshet[1,†]

SUMMARY

The angiogenic factor vascular endothelial growth factor A (VEGF) has been shown to have a role in neurogenesis, but how it affects adult neurogenesis is not fully understood. To delineate a role for VEGF in successive stages of olfactory bulb (OB) neurogenesis, we used a conditional transgenic system to suppress VEGF signaling at the adult mouse sub-ventricular zone (SVZ), rostral migratory stream (RMS) and OB, which constitute the respective sites of birth, the migration route, and sites where newly born interneurons mature and integrate within the existing OB circuitry. Following the development of fluorescently tagged adult-born neurons, we show that sequestration of VEGF that is constitutively expressed by distinct types of resident OB neurons greatly impaired dendrite development in incoming SVZ-born neurons. This was evidenced by reduced dendritic spine density of granule cells and significantly shorter and less branched dendrites in periglomerular neurons. Notably, the vasculature and perfusion of the SVZ, RMS and OB were not adversely affected when VEGF suppression was delayed until after birth, thus uncoupling the effect of VEGF on dendritogenesis from its known role in vascular maintenance. Furthermore, a requirement for VEGF was specific to newly born neurons, as already established OB neurons were not damaged by VEGF inhibition. This study thus uncovered a surprising perfusion-independent role of VEGF in the adult brain, namely, an essential role in the maturation of adult-born neurons.

KEY WORDS: VEGF (VEGFA), Adult neurogenesis, Angiogenesis, Mouse

INTRODUCTION

Vascular endothelial growth factor (VEGF; VEGFA – Mouse Genome Informatics) is the key factor promoting and coordinating most, if not all, processes of blood vessel formation in the embryo and adult. In addition to its angiogenic role, VEGF is also important for maintaining vascular homeostasis by way of adjusting the vasculature to meet dynamic changes in oxygen supply and demand, controlling vascular permeability, and maintaining certain organ-specialized vascular phenotypes (e.g. the blood-brain barrier or endothelial fenestrations). Functions of this pleiotropic factor, however, extend beyond the vascular system and include essential roles in hematopoiesis, bone formation, hepatocyte proliferation and others (for a review, see Ferrara, 2004). An increasing body of evidence implicates VEGF in neuronal processes in the adult brain. Ectopic VEGF augments proliferation of adult hippocampal neurons and enhances hippocampus-dependent learning (Cao et al., 2004; Jin et al., 2002; Schanzer et al., 2004). Conversely, inhibition of VEGF abolishes the increase in basal neurogenesis that takes place in response to exercise or an enriched environment (Cao et al., 2004; Fabel et al., 2003). Neurogenesis was also shown to increase in the adult sub-ventricular zone (SVZ) in response to VEGF (Jin et al., 2002; Schanzer et al., 2004). A specific neurogenic process in which the role of VEGF was further analyzed is the seasonal addition of new neurons to the high vocal center (HVC) of male songbirds (Louissaint et al., 2002). VEGF is also neuroprotective, as shown both in vitro (Jin et al., 2000; Matsuzaki et al., 2001) and in animal models of ischemic neuronal injury (Sun et al., 2003). Remarkably, hypoexpression of *Vegfa* in the spinal cord leads to neuronal cell death and the development of an amyotrophic lateral sclerosis (ALS)-like disease that can be rescued by exogenous VEGF (Azzouz et al., 2004; Lambrechts et al., 2003). VEGF has also been suggested to play a role in neuronal migration during brain development (Schwarz et al., 2004) or following injury (Wang et al., 2007) and has been shown to promote neuronal migration in vitro (Balenci et al., 2007).

Canonically, neurogenesis in the adult brain takes place in two niches: the subgranular zone of the hippocampus and the SVZ, which continuously supplies new interneurons to the olfactory bulb (OB). The latter niche is more suitable for discerning successive stages of the overall process in which VEGF might play a role, owing to the fact that neuronal birth, migration, differentiation and integration are spatially and temporally separated. Briefly, neuroblasts destined to become OB interneurons leave their respective sites of origin in the SVZ and migrate rostrally (tangential migration) along the rostral migratory stream (RMS). Upon reaching the OB, cells migrate radially and, upon reaching their destinations at the granule cell layer (GCL) or glomerular layer (GL), differentiate into granule cells (GCs) or periglomerular cells (PGNs), respectively, becoming fully functional interneurons (see Fig. 1C). Tangential migration in the mouse OB is completed within 2-7 days following cell division, radial migration within 5-7 days, and differentiation to GCs or PGNs within 2 or 4 weeks, respectively, from birth (Petreanu and Alvarez-Buylla, 2002). In the next period of 45 days, sensory inputs determine whether newly added interneurons will thrive or regress. Approximately 50% of newly integrated GCs survive beyond this critical period and function for ~100 additional days on average, prior to being replaced by new cells (Ninkovic et al., 2007; Petreanu and Alvarez-Buylla, 2002). Whereas adult-born GCs comprise a sustained fraction (10%) of all GCs, newly added PGNs have a better survival rate, resulting in a linear increase in their number, reaching 30% at the age of 9 months (Mizrahi et al., 2006; Ninkovic et al., 2007). Others have reported that the population of newborn GCs increases with time to reach ~60% at the age of 12 months (Imayoshi et al., 2008).

[1]Department of Molecular Biology, Hadassah Medical School and [2]Department of Neurobiology, Institute for Life Sciences, The Hebrew University of Jerusalem, 91120 Jerusalem, Israel.

*These authors contributed equally to this work
†Authors for correspondence (mizrahia@cc.huji.ac.il; keshet@cc.huji.ac.il)

Accepted 5 November 2009

The processes of neuronal proliferation, migration, differentiation and survival are governed by complex cues that are mediated by both intrinsic and extrinsic factors that only recently started to be revealed (reviewed by Lledo et al., 2006). Here, we found that *Vegfa* is constitutively expressed in the OB in a unique spatial pattern that cannot be simply explained by its known vascular roles, which prompted us to examine a possible role for VEGF in OB adult neurogenesis. Using a bi-transgenic mouse system that we devised for conditional knockdown of VEGF signaling in the relevant regions of the adult brain, we indeed uncovered an unexpected role of VEGF in the maturation of adult-born neurons.

MATERIALS AND METHODS

Animals

All animal procedures were approved by the animal care and use committee of the Hebrew University. Transgenic mouse lines used in this study were as follows. The *CamKIIα-tTA* brain-specific driver line was purchased from Jackson Labs (Mayford et al., 1996). *Vegfa-lacZ*-KI reporter was a generous gift of A. Nagy (Miquerol et al., 1999). *Flk1-lacZ*-KI reporter was a generous gift of J. Rossant (Shalaby et al., 1997). The pTet-sVEGF-R1 responder line was as described previously (May et al., 2008). For switching off I-sVEGF-R1, water was supplemented with 500 mg/l tetracycline (Tevacycline, Teva) and 3% sucrose. For switching on the transgene, tetracycline-supplemented water was replaced with fresh water for the desired time. BrdU (Sigma, 100 mg/kg body weight) was injected intraperitoneally for the durations indicated. Pimonidazole (Hypoxyprobe, Chemicon, 60 mg/kg body weight) was injected intraperitoneally 30 minutes prior to sacrifice. Dextran-FITC (MW 500,000, Sigma) was injected into the tail vein 5 minutes prior to sacrifice (2 mg per mouse).

Lentivirus, retrovirus and stereotaxic injection

Subventricular zone virus injection was as described (Mizrahi, 2007). Briefly, a commercial lentivirus (TranzVector, Tranzyme) or Moloney murine retrovirus (a generous gift of Carlos Lois, Picower Institute of Learning and Memory, MIT, Cambridge, MA, USA), both expressing GFP, were used to label newborn neurons. Mice were anaesthetized and a skull hole was drilled overlying the SVZ (coordinates relative to bregma: anterior, –1 mm; lateral, –1 mm; depth, 2.2 mm). Each mouse received two injections (~0.75 μl) on both the left and right SVZ. For histological analysis, mice were sacrificed, perfused with 4% paraformaldehyde and processed as described below.

Two-photon imaging and analysis

Obs were fixed with 1% paraformaldehyde, rinsed in 30% sucrose and dissected to 350 μm coronal sections. Imaging was carried out on an Ultima microscope (Prairie Technologies, Middleton, WI, USA) equipped with a 40× (0.8 NA) LUMPlan F1 water-immersion objective (Olympus). A femtosecond laser (Mai-Tai Spectra Physics) was used to excite GFP at 900 nm. Images (512 × 512 pixels) were acquired at 0.25 μm/pixel resolution in the *xy* dimension and in 0.9-1 μm steps in the *z* dimension. Reconstructions were carried out strictly on the raw data images. Reconstructions were performed manually from the complete three-dimensional image stacks using Neurolucida (MicrobrightField, Colchester, VT, USA). Quantitative parameters included the number of branch points and total dendritic branch length. Since 350 μm-thick slices were used, we could not assure that the whole dendritic tree was captured. In addition, in fixed slices the quality of the optical signal normally deteriorates when imaging deeper than 175 μm from the surface. For these two reasons, our data (although composed of a consistent sample) do not capture the complete dendritic tree. Notably, all reconstructions were conducted blind to the experimental group.

RNA in situ hybridization

In situ hybridization of formalin-fixed, paraffin-embedded tissue sections with ^{35}S-labeled antisense riboprobes was performed as described (Dor et al., 2001).

Immunohistochemistry

Formalin-fixed, paraffin-embedded tissues were dissected to 3 μm sections. Staining was performed with the following: anti-VEGFR1 (1:100, Santa Cruz), anti-BrdU (1:100, Amersham), anti-NRP1 (1:50, R&D), anti-NRP2 (1:100, Cell Signaling), anti-CD31 (1:50, BD Pharmingen), anti-VEGF (1:100, Calbiochem), anti-p44/42 (1:200, Cell Signaling), Hypoxyprobe (1:100, Chemicon) and anti-cleaved caspase 3 (1:100, Cell Signaling). The secondary reagents used were: Cy3 anti-goat, biotin anti-rat and Cy5 streptavidin (Jackson ImmunoResearch), Alexa-555 anti-rabbit (Invitrogen), FITC anti-mouse (Zymed) and ImmPress Universal (Vector Laboratories).

For BrdU-NeuN immunostaining, frozen 50 μm sections were pretreated with 50% formamide/2×SSC (0.3 M NaCl, 0.03 M sodium citrate) followed by 2 M HCl and 0.1 M boric acid. Incubation with rat anti-BrdU (1:200, Serotec) and mouse anti-NeuN (1:400, Chemicon) was followed by biotinylated rabbit anti-rat (Vector Laboratories), Cy5-conjugated extravidin and Cy3 anti-mouse (Jackson ImmunoResearch). Confocal microscopy was performed using a Nikon Eclipse 9i. *z*-stacks were done using a ×60 oil-immersion objective and 0.5 μm steps.

X-Gal staining

Tissue was fixed with 4% paraformaldehyde for 15 minutes on ice and then washed twice in rinse solution (PBS containing 2 mM $MgCl_2$, 0.01% sodium deoxycholate and 0.02% Nonidet P40). Staining was by incubation overnight at 37°C with rinse solution containing 5 mM ferrocyanide, 5 mM ferricyanide and 1 mg/ml X-Gal.

RESULTS

VEGF is constitutively expressed in three types of OB neurons, whereas VEGF receptors are mostly expressed in nearby endothelial cells.

To determine whether *Vegfa* is naturally expressed in the SVZ-RMS-OB axis and to identify *Vegfa*-expressing cells, we examined brain sections from adult (2-3 months old) mice harboring a *Vegfa* promoter-*lacZ* reporter transgene. In this mouse strain, a *lacZ* cassette has been inserted into the 3′UTR of the endogenous *Vegfa* gene such that β-galactosidase (β-gal) activity faithfully recapitulates natural patterns of *Vegfa* expression (Miquerol et al., 1999). Patterns of *Vegfa* expression were also determined by mRNA in situ hybridization and immunostaining using a specific riboprobe and antibodies, respectively. In the SVZ, *Vegfa* expression was evident as weak and diffuse β-gal staining or as a weak mRNA in situ signal. By comparison, the adjacent choroid plexus was strongly labeled, as described previously (Breier et al., 1992) (see Fig. S1 in the supplementary material). In the RMS, *Vegfa* expression was not detected by any of three detection methods (see Fig. S1 in the supplementary material). Remarkably, a unique spatial pattern of *Vegfa* expression was evident in the OB, mostly distributed in two concentric cell layers (Fig. 1A,B). *Vegfa*-expressing cells were subsequently identified as mitral cells within the inner layer and as juxtaglomerular cells (tufted and periglomerular cells) within the outer cell layer (Fig. 1A, middle, Fig. 1C). In the GCL, *Vegfa* was also expressed by some astrocytes, as evident by co-immunostaining with GFAP (Fig. 1A, right). This unique pattern of expression was unlikely to merely reflect a vascular maintenance function of VEGF, as in that case *Vegfa* would have been expected to be more uniformly expressed within the OB, rather than being restricted to these specific locales. The finding that the four types of VEGF-producing cells reside close to destination sites of incoming new neurons (see Fig. 1D) prompted us to examine a possible role for VEGF in neuronal maturation or integration.

As a prelude to examining a putative role for VEGF in neuronal maturation, we wished to determine which cells within the OB might respond to the constitutively expressed VEGF by virtue of

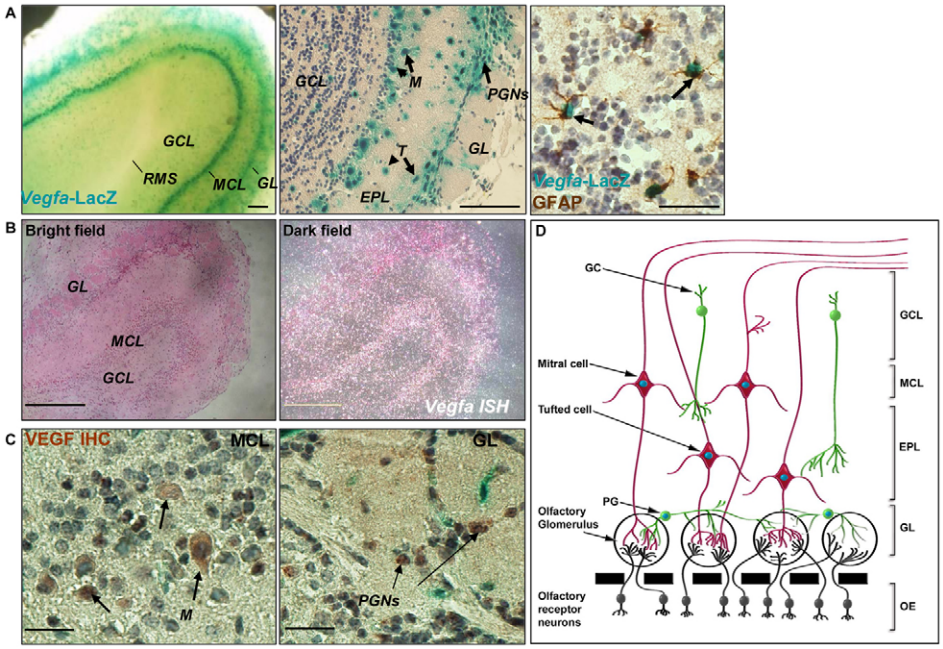

Fig. 1. *Vegfa* expression in the adult olfactory bulb. (**A**) Endogenous *Vegfa* expression in the adult brain is demonstrated using a transgenic mouse in which a *lacZ* reporter was inserted to the 3′UTR of the *Vegfa* gene. (Left) Coronal whole-mount view of the OB. Scale bar: 50 μm. (Middle) Hematoxylin and Eosin (H&E) staining of a coronal section of the OB. X-Gal staining (blue) is seen mostly in mitral, tufted and periglomerular cells. Note the absence of *Vegfa* in the RMS. Scale bar: 50 μm. (Right) *Vegfa*-expressing cells in the GCL (arrows) co-expressing GFAP and with astrocyte-like morphology. Scale bar: 20 μm. (**B**) ISH for *Vegfa*. Note the intense hybridization in the MCL and GL, consistent with the pattern revealed by the *Vegfa* transgenic reporter above. Scale bars: 200 μm. (**C**) Immunohistochemistry for VEGF in the OB showing immunoreactive cells in the MCL and GL (brown). Arrows indicate cells with morphology typical of mitral cells (left) and PGNs (right). Scale bars: 20 μm. (**D**) Schematic of OB neurons. Adult-born cells are highlighted in green. *Vegfa*-expressing cells are marked by a blue nucleus. OB, olfactory bulb; RMS, rostral migratory stream; GC, granule cell; PGN, periglomerular neuron; M, mitral cell; T, tufted cell; OE, olfactory epithelium; GL, glomerular layer; EPL, external plexiform layer; MCL, mitral cell layer; GCL, granule cell layer; IHC, immunohistochemistry; ISH, in situ mRNA hybridization.

expressing VEGF receptors. Considering that VEGFR2 (*Flk1*; *Kdr* – Mouse Genome Informatics) was previously shown to be expressed on neural cells both in vitro (Jin et al., 2006) and in vivo (Jin et al., 2002; Krum et al., 2002) and to mediate certain neuronal functions (Jin et al., 2002; Maurer et al., 2003), we first examined its pattern of expression by mRNA in situ hybridization (ISH) and through the use of an *Flk1* promoter-*lacZ* reporter mouse (Shalaby et al., 1997). Consistent with previous studies (Schanzer et al., 2004), *Flk1* expression was indeed detected by both methods in neuroepithelial cells of the SVZ ependyma and in the choroid plexus (see Fig. S2 in the supplementary material). In the OB proper, however, *Flk1* expression was only detected on endothelial cells residing in the GCL and GL, but not on neuronal cells or astrocytes in the same layers (see Fig. 2A,B). A similar analysis was extended to VEGFR1 (*Flt1*), previously reported to be expressed in astrocytes of the SVZ and RMS (Krum et al., 2002; Wittko et al., 2009). Focusing on the OB proper, however, a *Flt1* ISH signal was only detected in endothelial cells of the GL and GCL layers, but not in neurons or astrocytes in the same regions (Fig. 2C).

Next, we determined patterns of OB expression of neuropilin 1 (*Nrp1*) and neuropilin 2 (*Nrp2*) by in situ immunostaining. Consistent with previously reported patterns (Cloutier et al., 2002), olfactory sensory neuron (OSN) axons were found to be strongly immunoreactive. However, no expression was detected in endothelial cells or in GCs or PGNs within the OB (Fig. 2D,E). Together, these results suggest that neuronal cells within the OB might not be directly responsive to VEGF (see Discussion).

A transgenic system for conditional knockdown of VEGF in the SVZ-RMS-OB axis

To examine a possible role for VEGF in successive stages of OB neurogenesis, we devised a transgenic system to conditionally knockdown VEGF signaling at the relevant regions of the adult brain. The system is based on conditional induction and, in turn, de-induction of a secreted VEGF decoy receptor. Briefly, transgenic mice expressing a tetracycline-regulated transactivator protein (tTA) from a calmodulin kinase IIα (*CamKIIα*; *Camk2a* – Mouse Genome Informatics) promoter (Mayford et al., 1996) were mated with transgenic mice harboring a transgene encoding a chimeric tetracycline-regulated protein comprising an IgG1-Fc tail fused to the five Ig-like loops of the extracellular domain of VEGFR1. The induced secreted receptor (abbreviated as I-sVEGF-R1) efficiently binds and sequesters VEGF, thereby precluding its signaling (Kendall et al., 1996) (see Fig. 3A).

In all experiments described below, double-transgenic mice were selected for VEGF modulations, whereas littermates that inherited only one of the two transgenes served as controls. The onset of I-sVEGF-R1 activation in double-transgenic animals and the duration of its expression were tightly controlled by including or omitting tetracycline from the drinking water (‘off’ and ‘on’ modes, respectively) (Fig. 3A,B).

Under the dictate of the *CamKIIα* promoter, which was chosen because of its increased activity in brain areas of increased plasticity, I-sVEGF-R1 was robustly induced upon tetracycline withdrawal in the SVZ, RMS and in the GCL and GL layers of the OB, i.e. in the

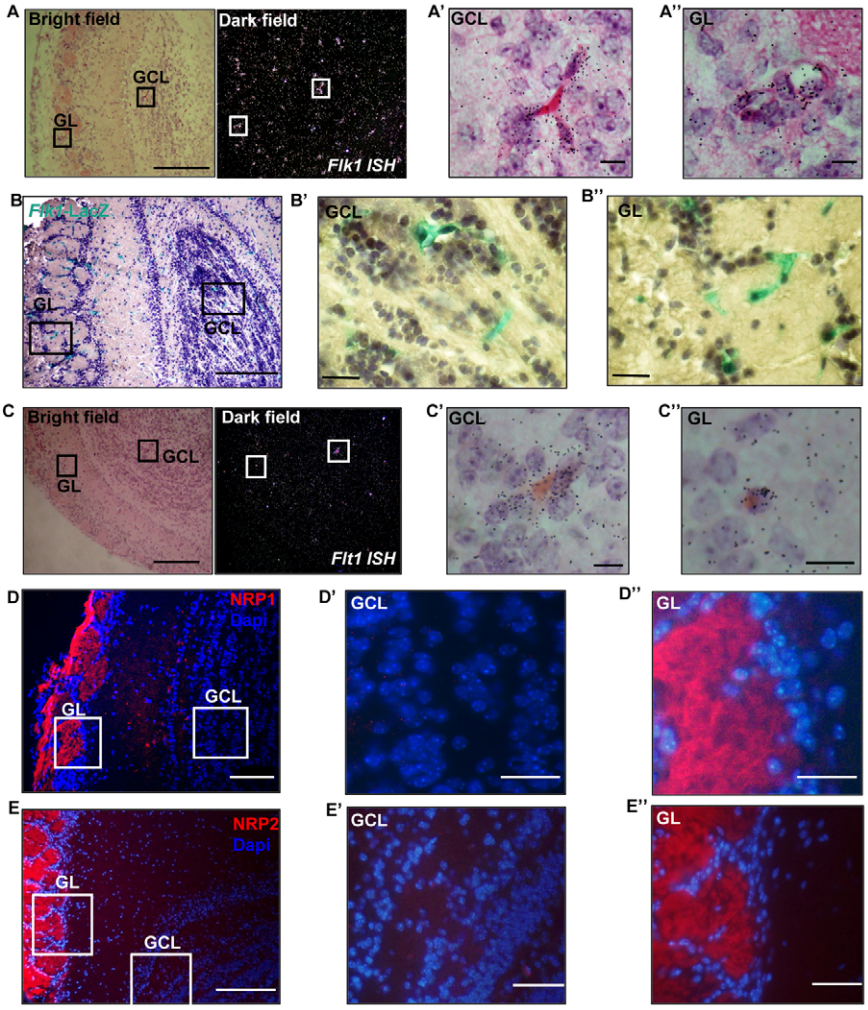

Fig. 2. Patterns of expression of VEGF receptors in the OB. (**A-B″**) *Flk1*. (A) ISH with a *Flk1*-specific riboprobe. (A′,A″) Higher magnification of the boxed regions in A, showing hybridization signals in erythrocyte-containing capillaries in the GCL and GL. (B) *Flk1* expression highlighted using the *Flk1-lacZ* transgenic reporter mouse. (B′,B″) Representative *lacZ*-positive cells in the GCL and GL shown at higher magnification. All *lacZ*-positive cells exhibit endothelial cell morphology. (**C-C″**) *Flt1* mRNA ISH. Note the hybridization signal in erythrocyte-containing capillaries. (C′,C″) Representative capillaries in the GCL and GL shown at higher magnification. (**D-E″**) Immunostaining for NRP1 (D-D″) and NRP2 (E-E″). OB glomeruli are immunoreactive, whereas endothelial cells, GCs and PGNs are not. Scale bars: 200 μm in A-E; 50 μm in E′,E″; 10 μm in B′,B″,C′,C″; 20 μm in A′,A″,D′,D″.

respective sites of neurogenesis, neuronal migration and neuronal maturation and integration (Fig. 3B,C). I-sVEGF-R1 was also strongly induced in olfactory glomeruli formed by coalescence of OSN axons. Indeed, intense I-sVEGF-R1 immunoreactivity was found in OSN cell bodies in the olfactory epithelium (Fig. 3C, right). The *CamKIIα* promoter also drove I-sVEGF-R1 expression in additional areas of the adult brain, such as in the cortex and hippocampus, although areas outside the SVZ-RMS-OB axis were not examined in this study. Importantly, the induced VEGF-sequestering receptor is a secreted protein such that VEGF is efficiently titrated regionally, irrespective of the exact identity of the producer cell. This provided us with the opportunity to determine which process, if any, might require VEGF.

Uncoupling perfusion-dependent and -independent requirements for VEGF in the developing and adult brain

Uncovering non-vascular roles of VEGF using different methods of *Vegfa* inhibition, such as Cre-mediated deletion or using a hypomorphic *Vegfa* allele (Haigh et al., 2003; Raab et al., 2004), has been hampered by the fact that these procedures may negatively impact on tissue perfusion. It has been difficult, therefore, to rule out the possibility that observed phenotypes are merely a secondary consequence of hypoxia or nutrient deprivation or result from a deficit in other crucial circulating factors. For example, it is currently unknown whether the severe developmental brain defects in *Vegfa* hypomorphic mice (Haigh et al., 2003) reflect a non-vascular role of VEGF in the brain or are secondary to impaired perfusion. VEGF is known to be required not only for neovascularization, but also for sustaining newly formed vessels, which become refractory to VEGF only upon their maturation (Benjamin et al., 1999). We reasoned, therefore, that beyond a critical developmental period, VEGF blockade would no longer lead to vessel regression or to a compromised vascular function. To test this, we used the same *CamKIIα*-driven conditional system for inducing I-sVEGF-R1 in the mouse brain at different embryonic and postnatal days.

The severity of the resulting brain defects (e.g. the magnitude of cortical thinning and neuronal apoptosis) was indeed markedly reduced as the onset of VEGF inhibition was further delayed (data not shown). When the onset of I-sVEGF-R1 induction was delayed until embryonic day 13.5, animals survived to adulthood and gross brain abnormalities were no longer detected at birth. Yet, a continued VEGF blockade led to involution of the OB, culminating in rudimentary bulbs and even their total absence (Fig. 4). Inspection of bulbs undergoing involution revealed a significant vascular loss (Fig. 4C,D), widespread regions of tissue hypoxia [visualized by staining with an antibody against pimonidazole (Hypoxyprobe) that selectively marks hypoxic microenvironments] and extensive cell apoptosis (Fig. 4F,H). Premature VEGF withdrawal also led to collapse of the RMS vascular support, ensuing hypoxia and massive apoptosis of SVZ-born neurons along their migration route towards

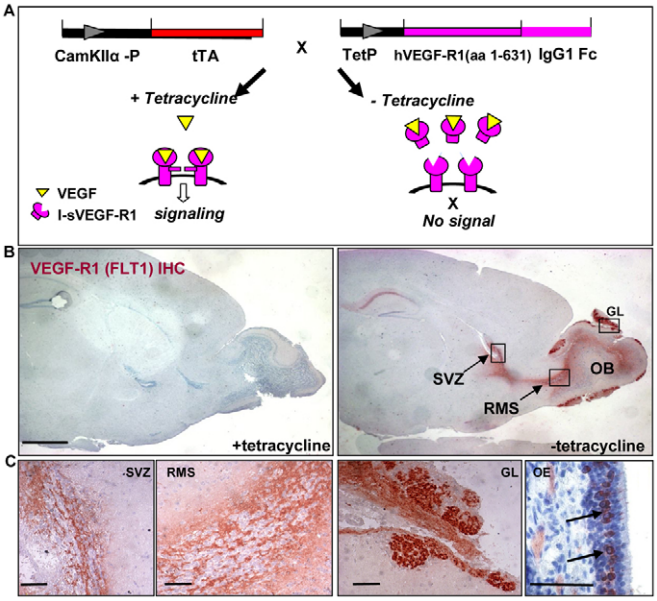

Fig. 3. Bi-transgenic conditional system for VEGF knockdown in the SVZ-RMS-OB pathway. (**A**) Schematic representation of the two transgenic mouse lines: the driver line (left) expressing tetracycline-regulated transactivator under the *CamKIIα* promoter and the responder line (right) expressing I-sVEGF-R1-Ig fusion protein under the *Tet* promoter. I-sVEGF-R1 is expressed in *CamKIIα*-positive cells upon withdrawal of tetracycline from the drinking water. (**B**) Expression of I-sVEGF-R1 in the forebrain is demonstrated by immunostaining for the extracellular domain of VEGFR1 (FLT1, brown). Sagittal sections of adult double-transgenic animals that were held on tetracycline (left) and fresh water (right) are presented. (**C**) High magnification images of the boxed areas in B. Strong expression in the glomeruli is a result of expression in olfactory sensory neurons (OSNs, arrows) within the olfactory epithelium (right). Scale bars: 2 mm in B; 50 μm in C.

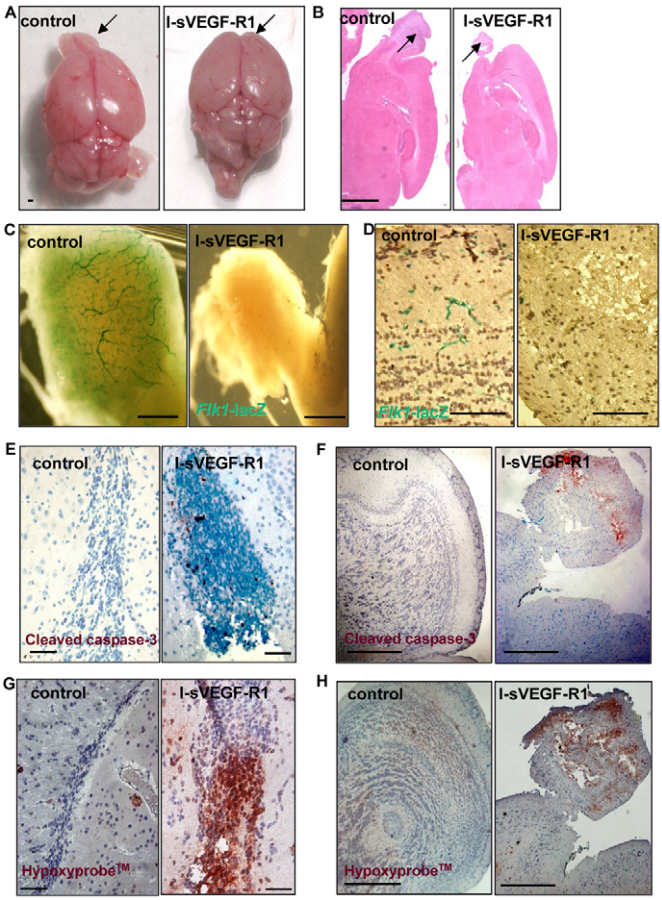

Fig. 4. VEGF loss-of-function in the embryo leads to vascular collapse, neuronal cell death and OB involution. Tetracycline-supplemented water was replaced by fresh water at embryonic day 13.5. Following intraperitoneal injection of pimonidazole (Hypoxyprobe), mice were sacrificed at P30. (**A**) Whole brains from control and I-sVEGF-R1 animals. Note the loss of the OB (arrows) in the I-sVEGF-R1 brain. (**B**) Saggital H&E-stained sections showing a degenerated rudimentary OB (right). (**C**,**D**) Low- and high-magnification images, respectively, of the OB showing loss of blood vessels in the degenerated OB of I-sVEGF-R1 animals. Vessels were visualized by *lacZ* staining in mice harboring an *Flk1-lacZ* knock-in transgene. (**E**) Cleaved caspase 3 staining (brown) of the RMS showing many apoptotic cells in the I-sVEGF-R1 mouse. Note the accumulation of migrating neuroblasts behind an abnormal cavity in the RMS. (**F**) Cleaved caspase 3 staining (brown) of the OB showing widespread areas of apoptosis in the rudimentary OB of the I-sVEGF-R1 mouse. (**G**) Hypoxyprobe staining of the RMS showing severe hypoxia in the I-sVEGF-R1 mouse. (**H**) Hypoxyprobe staining of the OB showing massive hypoxia in the I-sVEGF-R1 mouse. Scale bars: 1 mm in A-C; 200 μm in D; 500 μm in F,H; 100 μm in E,G.

the OB (Fig. 4E,G). In fact, as a result of the failure to cross the RMS, whether owing to the lack of a proper vascular scaffold or to the loss of their target, migrating neuroblasts piled up amidst the RMS and eventually died (Fig. 4E,G).

In sharp contrast to the VEGF dependence of the RMS and OB vasculatures at earlier times, delaying the onset of VEGF blockade until after birth no longer resulted in damage to the, by then, already mature vascular network anywhere along the SVZ-RMS-OB axis. When VEGF blockade was initiated in the adult brain (Fig. 5), no evidence for excessive endothelial or neuronal cell death was noted (as examined by immunostaining for cleaved caspase 3; Fig. 5A). More importantly, organ perfusion was not affected, as evidenced by CD31 (PECAM1 – Mouse Genome Informatics) immunostaining for endothelial cells in the RMS (Fig. 5C) and in the OB (Fig. 5D,F), as well as by tail vein injection of fluorescently tagged dextran, which revealed no change in the density and distribution of patent vessels (Fig. 5E,G). As expected, there was also no evidence for hypoxia (Fig. 5B). These findings allowed us to rigorously rule out the possibility that any of the neuronal OB phenotypes described below, as induced by VEGF inhibition at the indicated times after birth, might be secondary to a compromised perfusion.

We nevertheless wished to obtain a positive indication that inducing I-sVEGF-R1 in the adult does induce VEGF blockade in the OB and eventually leads to altered signaling in neuronal cells. To this end, we examined the phosphorylation status of p42/44 (ERK1/2 – Mouse Genome Informatics), a known downstream target of VEGF (Gliki et al., 2001) as well as of other neurogenic factors (Fu et al., 2002; Obrietan et al., 2002; Wu et al., 2007). Phosphorylation of p42/44 in GCs is induced by activity (odor stimulation) (Miwa and Storm, 2005). Switching on I-sVEGF-R1 in the adult brain for 3-6 weeks indeed led to a reduction in phospho-p42/44 in GCs from ~1000 to ~400 positive cells/mm^2 in the GCL area (see Fig. S3 in the supplementary material). We therefore conclude that VEGF loss-of-function (LOF) in the adult OB, although not adversely changing perfusion, may alter GC signaling, even though this is not necessarily via a direct mechanism.

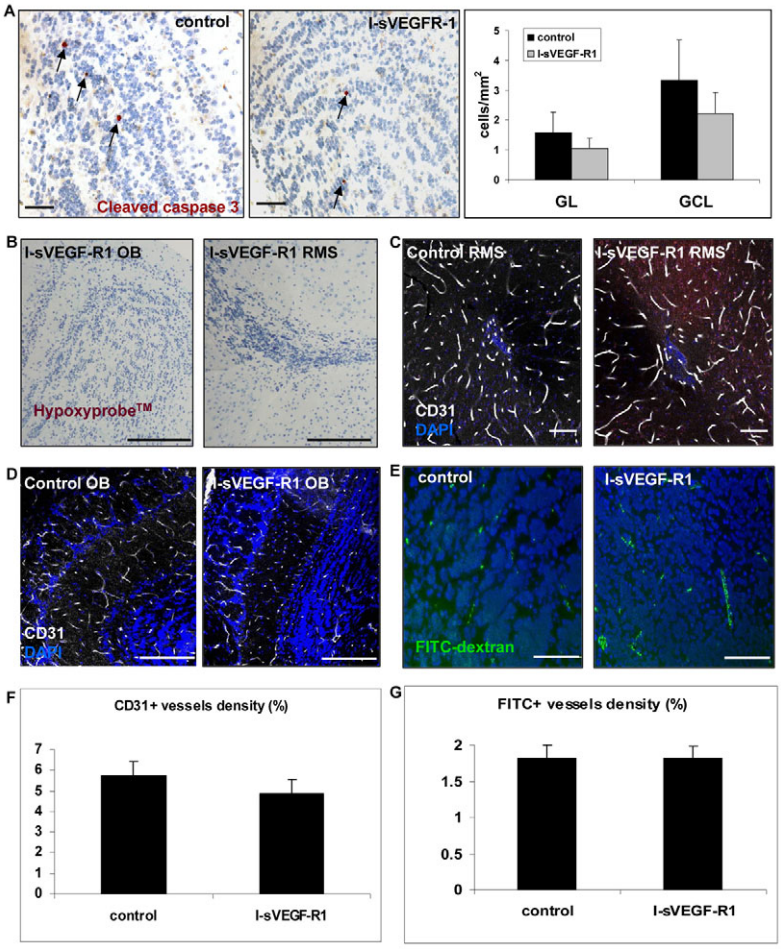

Fig. 5. Blood vessels in the adult RMS and OB are refractory to VEGF loss-of-function. I-sVEGF-R1 was induced in adult mice [postnatal day (P) 30 or older] for 30-60 days. Pimonidazole (Hypoxyprobe) was injected before sacrifice. (**A**) Cleaved caspase 3 immunostaining showing occasional positive cells (arrows) in the GCL. Quantification of cleaved caspase 3-positive cells (right) in the GL and GCL showing no significant difference between I-sVEGF-R1-induced and control animals. (**B**) Hypoxyprobe staining of OB and RMS from I-sVEGF-R1 mouse showing no evidence of hypoxia. (**C**) CD31 immunostaining for blood vessels showing normal vascular density and distribution in the RMS. (**D**) CD31 immunostaining showing normal vascular density and distribution in the OB. (**E**) OB sections following intravenous injections of FITC-dextran to highlight patent vessels. (**F**,**G**) Quantification of the relative area of CD31-positive (F, see D) or FITC-positive (G, see E) capillaries per field (n=4 per transgene, eight fields per animal counted, P>0.2, Student's t-test). Scale bars: 50 μm in A; 100 μm in C,E; 200 μm in B,D.

Influx of SVZ-born neurons into the OB and deployment therein are not affected by VEGF blockade

To identify a particular step in the overall process that might be compromised by VEGF inhibition, we first compared the number of newly born neurons that reach the OB using BrdU labeling experiments. I-sVEGF-R1 was induced in 2-month-old mice and 1 week later a short BrdU pulse was given. Animals were maintained in the 'on' mode for an additional 45 days to allow sufficient time for neuronal migration, maturation and integration and were then sacrificed for analysis. Newly added neurons were identified as cells double positive for BrdU and NeuN (NEUNA60 – Mouse Genome Informatics), and their numbers in the GCL and GL were compared with those detected in control littermates (see Fig. 6A for representative examples and Fig. 6C for quantification). A similar number of $BrdU^+/NeuN^+$ cells were detected in the GCL of control and VEGF-inhibited mice (663 and 611 cells/mm^2, respectively). Likewise, the number of newly added neurons was not significantly different in the GL of control and VEGF-inhibited mice (188 and 228 cells/mm^2, respectively).

Considering that the number of newly added neurons in the OB measures the net outcome of SVZ neurogenesis, migration through the RMS and survival, this result on its own does not rule out a role for VEGF in any of the individual processes. Nevertheless, the fact that the number of SVZ-born neurons reaching the OB and integrating therein was not reduced in the face of VEGF blockade enabled us to independently examine a putative role of VEGF in neuronal maturation.

VEGF inhibition leads to reduced dendritic spine density in newly acquired GCs

The finding of constitutive *Vegfa* expression in close proximity to integration sites of incoming neurons (Fig. 1) prompted us to examine a possible requirement for VEGF during the processes of neuronal maturation and integration. We first compared newly integrated GCs in control and VEGF-inhibited OBs with respect to their morphology. Briefly, I-sVEGF-R1 was induced in adult mice (with mono-transgenic littermates serving as controls), followed by SVZ injection of a lentivirus encoding green fluorescent protein (GFP) to tag SVZ-born neurons. OBs were retrieved for analysis 45 days later. Initial two-photon analysis of 350 μm-thick coronal sections did not reveal a significant difference in gross dendritic morphology of GCs (Fig. 7B). However, further analysis of 40 μm slices by confocal microscopy showed a marked decrease in the density of dendritic spines in mice that had been subjected to VEGF inhibition (Fig. 7C,D). Comparing the cumulative number of spines along dendritic segments exceeding 5 μm in length revealed that mice in which I-sVEGF-R1 was induced had only half the number of spines as control mice (0.21 versus 0.42 spines/μm, respectively). This reduction was also reflected in direct density measurements, where the average distance between adjacent spines was found to be significantly greater in VEGF-inhibited mice (Fig. 7D). We conclude that although VEGF is not required for GC dendritogenesis, it is required for proper development of the complete array of synaptic connections of these cells.

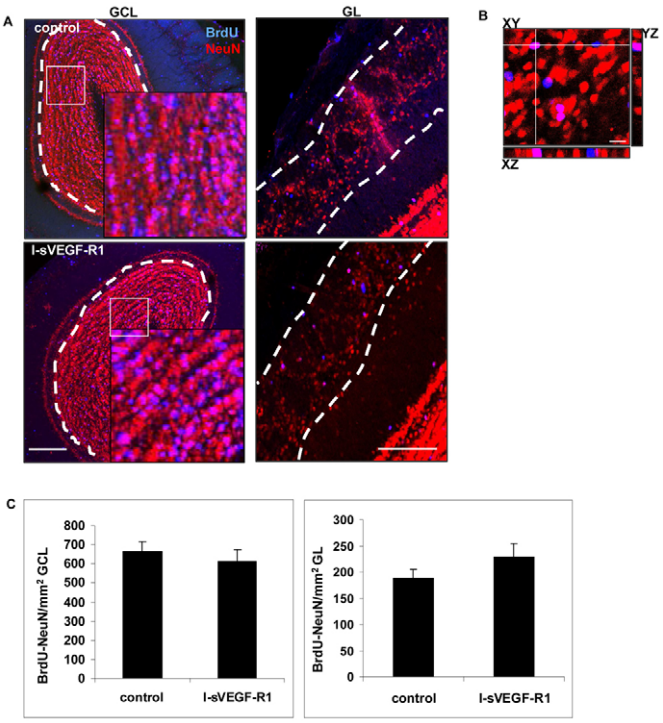

Fig. 6. VEGF is not essential for neuroblast migration, survival or distribution in the OB. BrdU (100 mg/kg body weight, four times at 4-hour intervals) was injected intraperitoneally to I-sVEGF-R1 adult (~P60) mice and their control littermates. I-sVEGF-R1 was switched on 1 week before BrdU injections. Animals were sacrificed 45 days later and 40 μm slices stained with anti-BrdU antibody (blue) and anti-NeuN antibody (red) to label newborn neurons. (**A**) Confocal image of bulbs from control and I-sVEGF-R1 animals. (Left) GCL, insets are an enlargement of framed areas; (right) GL. The relevant area is outlined (dashed line). Scale bars: 200 μm. (**B**) High-magnification confocal image of granule cells at three orthogonal planes demonstrating double labeling (purple) with BrdU and NeuN antibodies. Scale bar: 20 μm. (**C**) Quantification of double-labeled cells in the GCL and GL reveals no significant difference between control (n=12 bulbs) and I-sVEGF-R1 (n=10 bulbs). P>0.5, Student's t-test.

VEGF inhibition impairs dendritogenesis of newborn PGNs

A similar type of analysis to that described above for GCs was extended to the more peripheral PGNs. GFP-expressing PGNs were imaged in thick slices by two-photon microscopy. This allowed us to capture the dendritic trees of newly added PGNs, which were then reconstructed in 3D. PGNs from VEGF-inhibited mice displayed markedly fewer developed dendritic trees than control mice (Fig. 7E). This was evidenced by a 2-fold reduction in total dendritic length (364.8 μm compared with 762.9 μm in controls) (Fig. 7F, left), as well as significant reduction in the number of dendritic branching points (3.2 compared with 9.3 in controls) (Fig. 7F, right; but see reservations it terms of whole-cell morphology in Materials and methods). These results indicate that VEGF is required for proper dendritogenesis of adult-born PGNs.

Dendritogenesis of established GCs and PGNs is not impaired by VEGF inhibition

We next wished to determine whether VEGF is also required for the maintenance of dendritic spines in mature GCs and for the maintenance of proper dendritic trees of mature PGNs. We turned

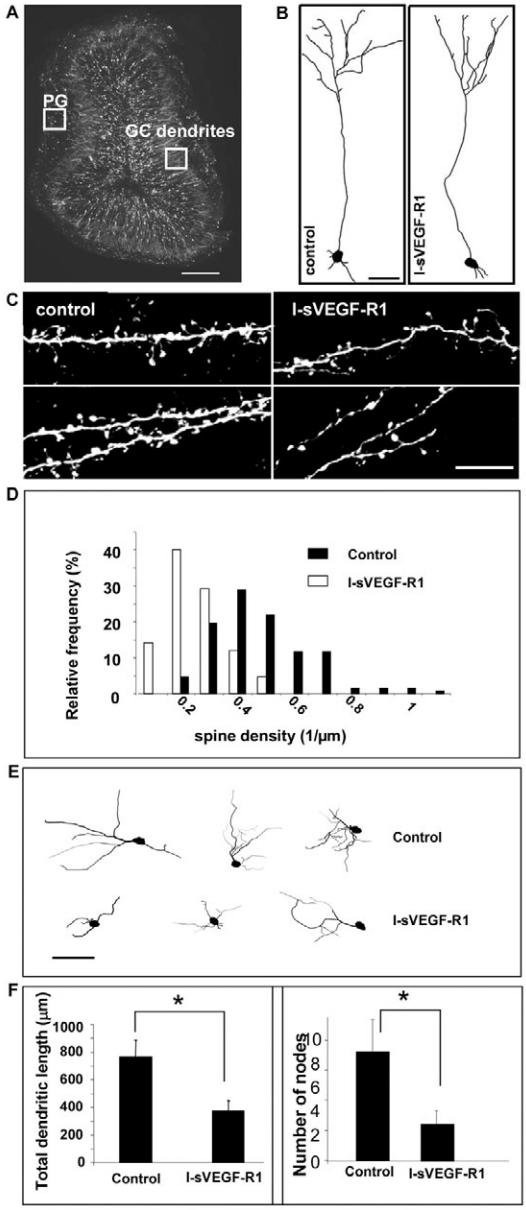

Fig. 7. I-sVEGF-R1 induction reduces the spine density of newborn GCs and the dendritic length and nodes of newborn PGNs. GFP-expressing lentivirus was injected into the SVZ of adult (~P60) mice and analysis performed 45 days later (i.e. following cell maturation). I-sVEGF-R1 was switched on 1 week before viral injection. (**A**) Representative image of the OB showing the fields analyzed for quantification of dendritic morphology of GCs and PGNs. Scale bar: 500 μm. (**B**) GFP-expressing GC dendritic trees from control and I-sVEGF-R1 animals. A 3D reconstruction of 350 μm slices is shown. Scale bar: 20 μm. (**C**) High-resolution confocal micrographs of GFP-expressing GCs within the EPL (third-order dendrites are shown). Representative images from control (left) and I-sVEGF-R1 (right) mice are shown. Scale bar: 20 μm. (**D**) Spine density distributions of newborn GC dendritic fragments from I-sVEGF-R1 mice compared with controls (n=7 in the I-sVEGF-R1 group and n=6 in the control group, P<0.001, Student's t-test). (**E**) 3D reconstructions of PGNs from the OB of control and I-sVEGF-R1 mice. Imaging was carried out on 350 μm slices of fixed tissue. Scale bar: 50 μm. (**F**) Quantification of the total dendritic length of PGNs (left) and the number of nodes (branching points) of PGNs (right). n=7 in the I-sVEGF-R1 group and n=6 in the control group, P<0.05, Student's t-test.

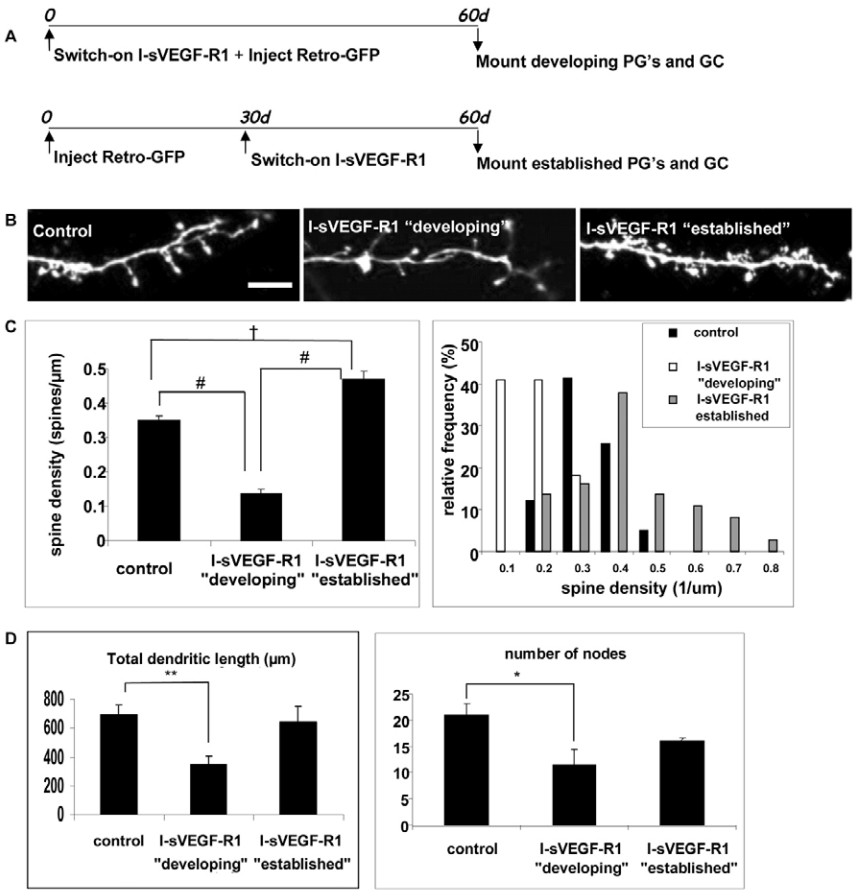

Fig. 8. VEGF is not essential for the maintenance of established PGNs and GCs. (**A**) Experimental design. Cells were mounted at 60 days post-injection of retrovirus encoding GFP. I-sVEGF-R1 was induced at the birth of cells to label developing cells and at day 30 (following their maturation within the OB) to label established cells. (**B**) Representative images of GC dendritic spines (third-order dendrites are shown). Scale bar: 20 µm. (**C**) Quantification of the average (left) and distribution (right) of spine density of GCs. (**D**) Total dendritic length and the number of nodes of PGNs. *n*=6 animals in the 'established' group, *n*=4 in the 'developing' group and *n*=10 in the control group. #, $P<0.0001$; †, $P<0.005$; **, $P<0.01$; *, $P<0.05$ of indicated groups (Student's *t*-test). All experiments were performed on adult (~P60) mice.

to SVZ injection of GFP-expressing retrovirus that allows for a more accurate birthdating of SVZ-born cells. Following the injection of a GFP-encoding retrovirus in the SVZ, animals were divided into two groups. In the first group, animals were kept in the 'off' mode for 30 days to allow sufficient time for integration and maturation of GFP-tagged incoming neurons. I-sVEGF-R1 was then switched 'on' for an additional 30 days, the OB resected and dendritic trees and spines analyzed as described above. In the second group, I-sVEGF-R1 was induced concomitantly with SVZ injection of the same GFP-encoding retrovirus and animals were maintained in the 'on' mode throughout the 60-day duration of the experiment (see Fig. 8A). This experiment allows adult-born neurons that were deprived of VEGF during development and onwards ('developing') to be distinguished from those deprived of VEGF after their maturation ('established'). In accordance with the results obtained with the lentivirus vector (Fig. 7, above), withdrawal of VEGF during development resulted in GCs with fewer dendritic spines and in PGNs with poorly developed dendritic trees (Fig. 8). By sharp contrast, no impairments of spine formation or dendritogenesis were detected when VEGF was withdrawn after maturation and integration of GCs and PGNs had taken place (Fig. 8). Further, VEGF knockdown at this stage of maturation resulted in a significant increase in GC spine density.

These results indicate that whereas VEGF is essential for normal spine formation and dendritogenesis of adult-born neurons, it is not required for maintaining already formed dendrites and spines. Nevertheless, the increase in spine density in VEGF-inhibited mature GCs suggests that it might have a role in those cells (see Discussion).

DISCUSSION

Vascular and neuronal cells may interact in different ways in the adult brain. Not only are constant adjustments of the vasculature required to match perfusion demands imposed by dynamic changes in neuronal activity, but the vasculature may also provide essential neurotrophic factors and participate in generating a proper niche for adult neurogenesis (Palmer et al., 2000; Shen et al., 2008; Tavazoie et al., 2008). Because VEGF is the key factor responsible for vascular homeostasis in the brain, it is also the prime candidate for a mediator of vascular/neuronal interactions and possibly also as a direct effector of non-vascular cells within the adult brain. VEGF has indeed been shown to enhance activity-induced hippocampal neurogenesis (Cao et al., 2004; Fabel et al., 2003). However, how VEGF might affect OB neurogenesis and which particular events in the neurogenic process might rely on VEGF remain unknown. Here, we uncovered a new and surprising role of VEGF in the maturation of OB interneurons. Specifically, VEGF is important for proper dendritogenesis of newly added PGNs and for dendritic spine formation of newly added GCs. Whether the new roles ascribed for VEGF by this study also apply to adult neurogenesis in the hippocampus, and perhaps even to general structural plasticity, remains to be determined.

Traditionally, it has been difficult to distinguish neuronal phenotypes resulting from impaired perfusion, which is an anticipated consequence of VEGF LOF, from perfusion-independent effects. The facility to conditionally knockdown VEGF in the adult brain in a highly localized and spatially restricted manner provided by our unique transgenic system allowed us to uncouple the two in the context of the natural in vivo setting. This is

particularly significant considering that different vascular beds within the brain may differ with regard of their dependency on VEGF. Furthermore, as demonstrated here for the RMS and OB vasculatures, the transition from a VEGF-dependent to a VEGF-independent phase may take place with a different developmental or postnatal timing. Clearly, our ability to exercise VEGF LOF only after securing that VEGF is no longer required for vascular maintenance (Fig. 5) is a prerequisite for exploring perfusion-independent functions of VEGF in the adult brain. Maintaining vascular integrity in the face of VEGF inhibition is also crucial in the context of the SVZ 'vascular niche of neurogenesis' and when utilizing blood vessels as a scaffold for neuronal migration in the OB (Bovetti et al., 2007).

Our results showing that adult VEGF blockade does not reduce the number of SVZ-born neurons entering the OB (Fig. 6) ought to be discussed with reference to studies demonstrating a role for VEGF in SVZ neurogenesis and in neuronal migration, as both are successive steps contributing to the overall process of populating the OB with new neurons. Previous studies that demonstrated enhanced proliferation of SVZ neurons by VEGF were based on VEGF gain-of-function (Jin et al., 2002; Wang et al., 2007), and currently there is no evidence for a natural role of endogenous VEGF in SVZ neurogenesis, despite high expression of *Flk1* in the ependyma (as confirmed here; see Fig. S2 in the supplementary material). Our results suggest, albeit not prove, that whereas vessels are needed for RMS migration (Bovetti et al., 2007), ongoing VEGF signaling might not be required. A requirement for VEGF signaling in neuronal migration has been elegantly demonstrated for the process of facial nerve development in which VEGF signaling was directly implicated in proper somata positioning (Schwarz et al., 2004). Yet, it remains to be determined whether VEGF also plays a direct role in neuroblast migration in the context of OB adult neurogenesis.

A comparable steady-state level of newly integrated neurons (Fig. 6) is compatible with the notion that VEGF is not required to sustain the survival of incoming neurons, a conclusion supported by our failure to detect increased cell death in the VEGF-inhibited OB (Fig. 5).

The fact that overall, sufficiently high numbers of SVZ-born neurons matured and integrated in the OB in the face of VEGF inhibition enabled us to uncover the roles of VEGF in dendritogenesis and dendritic spine formation. Whereas a number of proteins are known to promote dendritogenesis and synaptogenesis in adult-born cells in the dentate gyrus of the hippocampus (Danzer et al., 2008; Sato et al., 2007; Segura et al., 2007), almost nothing is known about factors that affect these processes in the OB, of which VEGF might be a first example.

In the adult hippocampus, VEGF has been shown to be involved in activity-induced neurogenesis but not to affect the rate of basal neurogenesis (Cao et al., 2004; Fabel et al., 2003). In the adult OB, it has been reported that environmental factors, such as odor deprivation by nostril occlusion, reduce GC dendritic spine density (Rehn et al., 1988; Saghatelyan et al., 2005). Interestingly, it was shown in these studies that odor deprivation only affects spine density in newborn GCs, and not in mature GCs. Our findings that VEGF sequestration results in reduced spine density in newborn, but not mature, GCs (Fig. 8) are also supported by a recent report describing a similar critical period for synaptic development of new GCs with respect to sensory inputs (Kelsch et al., 2009). Therefore, it is tempting to extrapolate that VEGF might mediate physiological responses to environmental changes. In fact, we found that whereas VEGF inhibition led to reduced dendritogenesis in developing cells, spine density in already mature cells was increased. Although we do not have a definitive explanation for this puzzling observation, several possibilities exist. First, GC dendritic spines are known to remain highly dynamic even after integration (Mizrahi, 2007) and VEGF might play a role in their continuous plasticity (such as in the control of spine pruning). Second, the increase in spine density of resident neurons might reflect an as yet unknown compensation mechanism for poor dendritogenesis of incoming new neurons. Third, this increase might reflect a compensation mechanism for other possible effects of VEGF inhibition in the OB that are yet to be discovered.

An open question concerns the functional consequences of the observed impediments to the maturation of new neurons in response to VEGF inhibition. A major effect is not expected in light of a recent report in which mice performed normally in several olfaction tasks despite genetic ablation of most interneurons (Imayoshi et al., 2008). Unexpectedly, however, in preliminary experiments we noticed compromised olfaction in VEGF-inhibited mice (data not shown), raising the possibility that, in addition to its effect on interneurons, VEGF might also be required for other cells participating in odor perception.

A basic unanswered question is whether the effects of VEGF on dendritogenesis are direct, i.e. take place via VEGF binding to neuronally expressed VEGF receptors, or indirect, i.e. via inducing endothelial cells or astrocytes to secrete another factor that acts on neuronal cells. A precedent for an indirect effect is the VEGF-induced seasonal addition of new neurons to the HVC of male songbirds (Louissaint et al., 2002). Here, testosterone-induced VEGF was found to stimulate nearby endothelial cells to secrete brain-derived neurotrophic factor (BDNF), which, in turn, promotes recruitment of neurons from the HVC ventricular zone. That neuronal cells may directly respond to VEGF is supported by expression of the high-affinity VEGF receptors VEGFR1 and VEGFR2 and of the auxiliary non-signaling receptors NRP1 and NRP2 on neuronal cells and on astrocytes (Jin et al., 2002; Jin et al., 2000; Mani et al., 2005; Maurer et al., 2003). We could not detect expression of any of the VEGF receptors on adult-born interneurons in the natural in vivo context (Fig. 2). Although we cannot exclude the possibility of low-level expression that is below our detection threshold, the data better argue for an indirect, paracrine effect of VEGF mediated by endothelial cells, which are shown here to express VEGF receptors. An autocrine VEGF effect on the resident neurons that produce it is yet another possibility, although autocrine VEGF effects have so far been described only in endothelial cells (Lee et al., 2007). Supporting a direct mechanism are findings showing that VEGF can induce neurite growth in cultured cortical neurons (Jin et al., 2006; Khaibullina et al., 2004; Rosenstein et al., 2003). In vivo, however, only the study of Schwarz et al., cited above in the context of migration, has convincingly demonstrated a direct action of VEGF on neuronal cell bodies (Schwarz et al., 2004). A rigorous distinction between direct and indirect mechanisms may necessitate neuronal-, glial- and endothelial-specific ablation (or functional knockdown in vivo) of each of the four VEGF signaling and auxiliary receptors. Whether direct or indirect, our findings clearly show that VEGF function is essential for proper development of the dendritic trees and dendritic spines specifically of maturing interneurons.

Acknowledgements

We thank Janet Rossant and Andras Nagy for mice and Carlos Lois for viral reagents. This study was supported by the Israel Science Foundation and the German-Israeli Foundation (to E.K.) and by a Career Development Award from the International Human Frontier Science Program Organization and the Abisch Frenkel Foundation (to A.M.).

Competing interests statement
The authors declare no competing financial interests.

Supplementary material
Supplementary material for this article is available at
http://dev.biologists.org/lookup/suppl/doi:10.1242/dev.039636/-/DC1

References

Azzouz, M., Ralph, G. S., Storkebaum, E., Walmsley, L. E., Mitrophanous, K. A., Kingsman, S. M., Carmeliet, P. and Mazarakis, N. D. (2004). VEGF delivery with retrogradely transported lentivector prolongs survival in a mouse ALS model. *Nature* **429**, 413-417.

Balenci, L., Saoudi, Y., Grunwald, D., Deloulme, J. C., Bouron, A., Bernards, A. and Baudier, J. (2007). IQGAP1 regulates adult neural progenitors in vivo and vascular endothelial growth factor-triggered neural progenitor migration in vitro. *J. Neurosci.* **27**, 4716-4724.

Benjamin, L. E., Golijanin, D., Itin, A., Pode, D. and Keshet, E. (1999). Selective ablation of immature blood vessels in established human tumors follows vascular endothelial growth factor withdrawal. *J. Clin. Invest.* **103**, 159-165.

Bovetti, S., Hsieh, Y. C., Bovolin, P., Perroteau, I., Kazunori, T. and Puche, A. C. (2007). Blood vessels form a scaffold for neuroblast migration in the adult olfactory bulb. *J. Neurosci.* **27**, 5976-5980.

Breier, G., Albrecht, U., Sterrer, S. and Risau, W. (1992). Expression of vascular endothelial growth factor during embryonic angiogenesis and endothelial cell differentiation. *Development* **114**, 521-532.

Cao, L., Jiao, X., Zuzga, D. S., Liu, Y., Fong, D. M., Young, D. and During, M. J. (2004). VEGF links hippocampal activity with neurogenesis, learning and memory. *Nat. Genet.* **36**, 827-835.

Cloutier, J. F., Giger, R. J., Koentges, G., Dulac, C., Kolodkin, A. L. and Ginty, D. D. (2002). Neuropilin-2 mediates axonal fasciculation, zonal segregation, but not axonal convergence, of primary accessory olfactory neurons. *Neuron* **33**, 877-892.

Danzer, S. C., Kotloski, R. J., Walter, C., Hughes, M. and McNamara, J. O. (2008). Altered morphology of hippocampal dentate granule cell presynaptic and postsynaptic terminals following conditional deletion of TrkB. *Hippocampus* **18**, 668-678.

Dor, Y., Camenisch, T. D., Itin, A., Fishman, G. I., McDonald, J. A., Carmeliet, P. and Keshet, E. (2001). A novel role for VEGF in endocardial cushion formation and its potential contribution to congenital heart defects. *Development* **128**, 1531-1538.

Fabel, K., Fabel, K., Tam, B., Kaufer, D., Baiker, A., Simmons, N., Kuo, C. J. and Palmer, T. D. (2003). VEGF is necessary for exercise-induced adult hippocampal neurogenesis. *Eur. J. Neurosci.* **18**, 2803-2812.

Ferrara, N. (2004). Vascular endothelial growth factor: basic science and clinical progress. *Endocr. Rev.* **25**, 581-611.

Fu, W., Lu, C. and Mattson, M. P. (2002). Telomerase mediates the cell survival-promoting actions of brain-derived neurotrophic factor and secreted amyloid precursor protein in developing hippocampal neurons. *J. Neurosci.* **22**, 10710-10719.

Gliki, G., Abu-Ghazaleh, R., Jezequel, S., Wheeler-Jones, C. and Zachary, I. (2001). Vascular endothelial growth factor-induced prostacyclin production is mediated by a protein kinase C (PKC)-dependent activation of extracellular signal-regulated protein kinases 1 and 2 involving PKC-delta and by mobilization of intracellular Ca2+. *Biochem. J.* **353**, 503-512.

Haigh, J. J., Morelli, P. I., Gerhardt, H., Haigh, K., Tsien, J., Damert, A., Miquerol, L., Muhlner, U., Klein, R., Ferrara, N. et al. (2003). Cortical and retinal defects caused by dosage-dependent reductions in VEGF-A paracrine signaling. *Dev. Biol.* **262**, 225-241.

Imayoshi, I., Sakamoto, M., Ohtsuka, T., Takao, K., Miyakawa, T., Yamaguchi, M., Mori, K., Ikeda, T., Itohara, S. and Kageyama, R. (2008). Roles of continuous neurogenesis in the structural and functional integrity of the adult forebrain. *Nat. Neurosci.* **11**, 1153-1161.

Jin, K. L., Mao, X. O. and Greenberg, D. A. (2000). Vascular endothelial growth factor: direct neuroprotective effect in in vitro ischemia. *Proc. Natl. Acad. Sci. USA* **97**, 10242-10247.

Jin, K., Zhu, Y., Sun, Y., Mao, X. O., Xie, L. and Greenberg, D. A. (2002). Vascular endothelial growth factor (VEGF) stimulates neurogenesis in vitro and in vivo. *Proc. Natl. Acad. Sci. USA* **99**, 11946-11950.

Jin, K., Mao, X. O. and Greenberg, D. A. (2006). Vascular endothelial growth factor stimulates neurite outgrowth from cerebral cortical neurons via Rho kinase signaling. *J. Neurobiol.* **66**, 236-242.

Kelsch, W., Lin, C. W., Mosley, C. P. and Lois, C. (2009). A critical period for activity-dependent synaptic development during olfactory bulb adult neurogenesis. *J. Neurosci.* **29**, 11852-11858.

Kendall, R. L., Wang, G. and Thomas, K. A. (1996). Identification of a natural soluble form of the vascular endothelial growth factor receptor, FLT-1, and its heterodimerization with KDR. *Biochem. Biophys. Res. Commun.* **226**, 324-328.

Khaibullina, A. A., Rosenstein, J. M. and Krum, J. M. (2004). Vascular endothelial growth factor promotes neurite maturation in primary CNS neuronal cultures. *Brain Res. Dev. Brain Res.* **148**, 59-68.

Krum, J. M., Mani, N. and Rosenstein, J. M. (2002). Angiogenic and astroglial responses to vascular endothelial growth factor administration in adult rat brain. *Neuroscience* **110**, 589-604.

Lambrechts, D., Storkebaum, E., Morimoto, M., Del-Favero, J., Desmet, F., Marklund, S. L., Wyns, S., Thijs, V., Andersson, J., van Marion, I. et al. (2003). VEGF is a modifier of amyotrophic lateral sclerosis in mice and humans and protects motoneurons against ischemic death. *Nat. Genet.* **34**, 383-394.

Lee, S., Chen, T. T., Barber, C. L., Jordan, M. C., Murdock, J., Desai, S., Ferrara, N., Nagy, A., Roos, K. P. and Iruela-Arispe, M. L. (2007). Autocrine VEGF signaling is required for vascular homeostasis. *Cell* **130**, 691-703.

Lledo, P. M., Alonso, M. and Grubb, M. S. (2006). Adult neurogenesis and functional plasticity in neuronal circuits. *Nat. Rev. Neurosci.* **7**, 179-193.

Louissaint, A., Jr, Rao, S., Leventhal, C. and Goldman, S. A. (2002). Coordinated interaction of neurogenesis and angiogenesis in the adult songbird brain. *Neuron* **34**, 945-960.

Mani, N., Khaibullina, A., Krum, J. M. and Rosenstein, J. M. (2005). Astrocyte growth effects of vascular endothelial growth factor (VEGF) application to perinatal neocortical explants: receptor mediation and signal transduction pathways. *Exp. Neurol.* **192**, 394-406.

Matsuzaki, H., Tamatani, M., Yamaguchi, A., Namikawa, K., Kiyama, H., Vitek, M. P., Mitsuda, N. and Tohyama, M. (2001). Vascular endothelial growth factor rescues hippocampal neurons from glutamate-induced toxicity: signal transduction cascades. *FASEB J.* **15**, 1218-1220.

Maurer, M. H., Tripps, W. K., Feldmann, R. E., Jr and Kuschinsky, W. (2003). Expression of vascular endothelial growth factor and its receptors in rat neural stem cells. *Neurosci. Lett.* **344**, 165-168.

May, D., Gilon, D., Djonov, V., Itin, A., Lazarus, A., Gordon, O., Rosenberger, C. and Keshet, E. (2008). Transgenic system for conditional induction and rescue of chronic myocardial hibernation provides insights into genomic programs of hibernation. *Proc. Natl. Acad. Sci. USA* **105**, 282-287.

Mayford, M., Bach, M. E., Huang, Y. Y., Wang, L., Hawkins, R. D. and Kandel, E. R. (1996). Control of memory formation through regulated expression of a CaMKII transgene. *Science* **274**, 1678-1683.

Miquerol, L., Gertsenstein, M., Harpal, K., Rossant, J. and Nagy, A. (1999). Multiple developmental roles of VEGF suggested by a LacZ-tagged allele. *Dev. Biol.* **212**, 307-322.

Miwa, N. and Storm, D. R. (2005). Odorant-induced activation of extracellular signal-regulated kinase/mitogen-activated protein kinase in the olfactory bulb promotes survival of newly formed granule cells. *J. Neurosci.* **25**, 5404-5412.

Mizrahi, A. (2007). Dendritic development and plasticity of adult-born neurons in the mouse olfactory bulb. *Nat. Neurosci.* **10**, 444-452.

Mizrahi, A., Lu, J., Irving, R., Feng, G. and Katz, L. C. (2006). In vivo imaging of juxtaglomerular neuron turnover in the mouse olfactory bulb. *Proc. Natl. Acad. Sci. USA* **103**, 1912-1917.

Ninkovic, J., Mori, T. and Gotz, M. (2007). Distinct modes of neuron addition in adult mouse neurogenesis. *J. Neurosci.* **27**, 10906-10911.

Obrietan, K., Gao, X. B. and Van Den Pol, A. N. (2002). Excitatory actions of GABA increase BDNF expression via a MAPK-CREB-dependent mechanism-a positive feedback circuit in developing neurons. *J. Neurophysiol.* **88**, 1005-1015.

Palmer, T. D., Willhoite, A. R. and Gage, F. H. (2000). Vascular niche for adult hippocampal neurogenesis. *J. Comp. Neurol.* **425**, 479-494.

Petreanu, L. and Alvarez-Buylla, A. (2002). Maturation and death of adult-born olfactory bulb granule neurons: role of olfaction. *J. Neurosci.* **22**, 6106-6113.

Raab, S., Beck, H., Gaumann, A., Yuce, A., Gerber, H. P., Plate, K., Hammes, H. P., Ferrara, N. and Breier, G. (2004). Impaired brain angiogenesis and neuronal apoptosis induced by conditional homozygous inactivation of vascular endothelial growth factor. *Thromb. Haemost.* **91**, 595-605.

Rehn, B., Panhuber, H., Laing, D. G. and Breipohl, W. (1988). Spine density on olfactory granule cell dendrites is reduced in rats reared in a restricted olfactory environment. *Brain Res.* **468**, 143-147.

Rosenstein, J. M., Mani, N., Khaibullina, A. and Krum, J. M. (2003). Neurotrophic effects of vascular endothelial growth factor on organotypic cortical explants and primary cortical neurons. *J. Neurosci.* **23**, 11036-11044.

Saghatelyan, A., Roux, P., Migliore, M., Rochefort, C., Desmaisons, D., Charneau, P., Shepherd, G. M. and Lledo, P. M. (2005). Activity-dependent adjustments of the inhibitory network in the olfactory bulb following early postnatal deprivation. *Neuron* **46**, 103-116.

Sato, K., Akaishi, T., Matsuki, N., Ohno, Y. and Nakazawa, K. (2007). beta-Estradiol induces synaptogenesis in the hippocampus by enhancing brain-derived neurotrophic factor release from dentate gyrus granule cells. *Brain Res.* **1150**, 108-120.

Schanzer, A., Wachs, F. P., Wilhelm, D., Acker, T., Cooper-Kuhn, C., Beck, H., Winkler, J., Aigner, L., Plate, K. H. and Kuhn, H. G. (2004). Direct

stimulation of adult neural stem cells in vitro and neurogenesis in vivo by vascular endothelial growth factor. *Brain Pathol.* **14**, 237-248.
Schwarz, Q., Gu, C., Fujisawa, H., Sabelko, K., Gertsenstein, M., Nagy, A., Taniguchi, M., Kolodkin, A. L., Ginty, D. D., Shima, D. T. et al. (2004). Vascular endothelial growth factor controls neuronal migration and cooperates with Sema3A to pattern distinct compartments of the facial nerve. *Genes Dev.* **18**, 2822-2834.
Segura, I., Essmann, C. L., Weinges, S. and Acker-Palmer, A. (2007). Grb4 and GIT1 transduce ephrinB reverse signals modulating spine morphogenesis and synapse formation. *Nat. Neurosci.* **10**, 301-310.
Shalaby, F., Ho, J., Stanford, W. L., Fischer, K. D., Schuh, A. C., Schwartz, L., Bernstein, A. and Rossant, J. (1997). A requirement for Flk1 in primitive and definitive hematopoiesis and vasculogenesis. *Cell* **89**, 981-990.
Shen, Q., Wang, Y., Kokovay, E., Lin, G., Chuang, S. M., Goderie, S. K., Roysam, B. and Temple, S. (2008). Adult SVZ stem cells lie in a vascular niche: a quantitative analysis of niche cell-cell interactions. *Cell Stem Cell* **3**, 289-300.
Sun, Y., Jin, K., Xie, L., Childs, J., Mao, X. O., Logvinova, A. and Greenberg, D. A. (2003). VEGF-induced neuroprotection, neurogenesis, and angiogenesis after focal cerebral ischemia. *J. Clin. Invest.* **111**, 1843-1851.
Tavazoie, M., Van der Veken, L., Silva-Vargas, V., Louissaint, M., Colonna, L., Zaidi, B., Garcia-Verdugo, J. M. and Doetsch, F. (2008). A specialized vascular niche for adult neural stem cells. *Cell Stem Cell* **3**, 279-288.
Wang, Y., Jin, K., Mao, X. O., Xie, L., Banwait, S., Marti, H. H. and Greenberg, D. A. (2007). VEGF-overexpressing transgenic mice show enhanced post-ischemic neurogenesis and neuromigration. *J. Neurosci. Res.* **85**, 740-747.
Wittko, I. M., Schanzer, A., Kuzmichev, A., Schneider, F. T., Shibuya, M., Raab, S. and Plate, K. H. (2009). VEGFR-1 regulates adult olfactory bulb neurogenesis and migration of neural progenitors in the rostral migratory stream in vivo. *J. Neurosci.* **29**, 8704-8714.
Wu, C., Ramirez, A., Cui, B., Ding, J., Delcroix, J. D., Valletta, J. S., Liu, J. J., Yang, Y., Chu, S. and Mobley, W. C. (2007). A functional dynein-microtubule network is required for NGF signaling through the Rap1/MAPK pathway. *Traffic* **8**, 1503-1520.